(1969).
[7]A. H. Gabriel and C. Jordan, Nature 221, 947 (1969).
[8]H. R. Griem, Astrophys. J. Letters 156, L103 (1969).
[9]A. I. Akhiezer and V. B. Berestetskii, *Quantum Electrodynamics* (Interscience, New York, 1965), pp. 347–353.
[10]A. Dalgarno and G. W. F. Drake, Chem. Phys. Letters 3, 349 (1969).
[11]G. W. F. Drake and A. Dalgarno, Phys. Rev. A 1, 1325 (1970).
[12]R. W. Schmieder and R. Marrus, Phys. Rev. Letters 25, 1245 (1970).
[13]M. Mizushima, Phys. Rev. 134, A833 (1964).
[14]H. A. Bethe and E. E. Salpeter, *Quantum Mechanics of One- and Two-Electron Atoms* (Springer, Berlin, 1957), p. 69.
[15]R. Karplus and N. M. Kroll, Phys. Rev. 77, 536 (1950); J. Schwinger, *ibid.* 82, 664 (1951).
[16]W. Perl and V. Hughes, Phys. Rev. 91, 842 (1953).
[17]L. L. Foldy and S. A. Wouthuysen, Phys. Rev. 78, 29 (1950).
[18]A. Messiah, *Quantum Mechanics* (Wiley, New York, 1962), Vol. II, pp. 944–946.
[19]A double-commutator relation with H_{NR} [cf. Eq. (34)] can be used to transform the term involving ω^2 with the result that (Ref. 25) $\langle 1\,^1S \mid Q_{10} \mid 2\,^3S\rangle = \mu_B \langle 1\,^1S \mid -(1/3m^2c^2)(p_1^2 - p_2^2) + (e^2/3mc^2)[(r_1^2 - r_2^2)/r_{12}^3] \mid 2\,^3S\rangle$. The above form does not involve ω and can be obtained directly from the operator derived by Perl and Hughes (Ref. 16 and earlier references therein) for the magnetic dipole moment of the $2\,^3S$ state of helium, even though their derivation applies only to a uniform static ($\omega = 0$) magnetic field. For computational purposes, Eq. (35) is more convenient since the r_{12} coordinate does not appear.
[20]C. W. Scherr and R. E. Knight, Rev. Mod. Phys. 35, 436 (1963).
[21]H. R. Griem has recently published an erratum giving the correct Z^{10} dependence for the M1 decay rate [Astrophys. J. Letters 161, L155 (1970)].
[22]F. F. Freeman, A. H. Gabriel, B. B. Jones, and C. Jordan, Proc. Roy. Soc. (London) (to be published); A. H. Gabriel and C. Jordan, Phys. Letters 32A, 166 (1970).
[23]H. A. Bethe and E. E. Salpeter, *Quantum Mechanics of One- and Two-Electron Atoms* (Springer, Berlin, 1957), p. 107.
[24]A. R. Edmonds, *Angular Momentum in Quantum Mechanics* (Princeton U. P., Princeton, N. J., 1960), p. 118.
[25]C. Schwartz (private communication).

PHYSICAL REVIEW A VOLUME 3, NUMBER 3 MARCH 1971

Measurements of Lowest-S-State Lifetimes of Gallium, Indium, and Thalium†

Michael Norton* and Alan Gallagher‡
Joint Institute for Laboratory Astrophysics, University of Colorado, Boulder, Colorado 80302
(Received 3 September 1970)

The lifetimes of the gallium $5\,^2S_{1/2}$ state, the indium $6\,^2S_{1/2}$ state, and the thallium $7\,^2S_{1/2}$ state were measured using the zero-field level-crossing (Hanle-effect) technique. The lifetimes obtained were $(6.8 \pm 0.3) \times 10^{-9}$, $(7.0 \pm 0.3) \times 10^{-9}$, and $(7.45 \pm 0.2) \times 10^{-9}$ sec, respectively. Anomalous contributions to the level-crossing signals, from the wavelength dependence of the exciting light intensity and self-absorption by the fluorescing atomic beam, were investigated in detail.

I. INTRODUCTION

A short time ago most measured or calculated atomic oscillator strengths were of uncertain reliability. Fortunately this situation is rapidly changing as a result of more numerous efforts and some different approaches. The increasing emphasis on direct lifetime measurements, rather than on oscillator strengths times vapor density, has freed the measurements from vapor-pressure and plasma-condition uncertainties. Increasing computer capabilities have allowed more sophisticated wave-function calculations. Almost as important, the available experimental and theoretical information is very efficiently utilized by Wiese and his collaborators,[1] who make extensive studies of regularities and consistencies.

At the moment, accurate lifetime measurements for the upper state of the principal resonance lines of the group-I and -II elements have been made by two independent techniques, level crossing or magnetic resonance and phase shift.[2-4] The agreements are almost all within the quoted experimental uncertainties, which are typically a few percent. A variety of relative oscillator-strength measurements, which are independent of vapor density, can be normalized to these resonance-line values to provide an impressive number of reliable oscillator strengths for these elements.[1] The measurements reported here allow several of the group-III elements to arrive in this same category of reliability. For these group-III elements as well, many relative values can be tied down with a single good lifetime measurement, while the lifetimes measured

here have also been recently measured by the phase-shift method.[4,5] The agreement between these and our level-crossing lifetime determinations is not always as good as for the group-I and -II elements, but it is good enough to instill a satisfactory confidence in the experiments. The accuracy of these measurements and the reasonable agreement with the phase-shift measurements also remove uncertainties in laboratory data as a significant contributor to uncertainties in these particular stellar abundances.[6] For several reasons, these group-III level-crossing experiments appear to be more difficult than those with the group-I and -II elements. In particular, the potential for systematic error appears much greater in the group-III measurements, and a very thorough study was required here to arrive at the usual error brackets of a few percent.

Another interesting feature of the measurements reported here is related to the fact that the fluorescing vapor was an atomic beam. The resulting narrowing of the Doppler absorption profile in the plane transverse to the beam has a number of important implications in level-crossing lifetime measurements. In particular, it can very easily lead to anomalous results in $\Delta m = 2$ level-crossing experiments with linearly polarized light. In this case the absorption effects have the same symmetry as the level-crossing signals and they cannot be separately observed by removing polarizers. Fortunately, the level-crossing signals are always undistorted in the zero-vapor-density limit, but this limit is only obtained at unusually small densities and of course in the limit of zero S/N. The present experiments involved $\Delta m = 1$ level crossing, so that the anomalous contributions to the signal could be more readily evaluated. Detailed comparisons and measurements were made to ensure the accuracy of the present measurements in spite of the signal-distorting effects. The high degree of self-consistency and the agreement of experimental and theoretical line shapes in spite of these effects is very gratifying. Indeed, the potential of level-crossing measurements for much more accurate lifetime measurements appears very good on the basis of such results from careful analyses. Our approach of directly adding errors and not bothering to accurately control magnetic fields and experimental drifts can easily be improved upon if the need arises. It appears that the effects of the lamp spectrum remain the most difficult, but not insurmountable, obstacle to measurements of fractional-percent accuracy.

II. THEORY

The lifetime determinations, using zero-field level crossing, depend upon measurements of the magnetic field dependence of the intensity of resonance fluorescence. For these experiments with $J = \frac{1}{2}$ excited states, one must excite with and detect circularly polarized light to observe the level crossings. If this is done with 90° scattering in the plane perpendicular to the magnetic field, then the Breit formula[7] with the linear Zeeman approximation predicts that the detected intensity varies with the field as $y/(1+y^2)$, where

$$y = g_J \mu_B H \tau/(2I+1)\hbar \, .$$

The experimentally determined fields at which $y = 1$, which we will call $\frac{1}{2}H_{1/2}$, can thus be used in conjunction with the known g_J to calculate the lifetimes τ. A number of phenomena can cause the experimentally detected intensity to vary from this basic form; these and the relevant evaluations using the Breit formula will now be discussed.

The general expression describing the intensity of the resonance radiation emitted from free atoms excited by "white light" was first obtained by Breit; in the notation of Franken[7] it is

$$R(f,g) = C \sum_{\mu\mu' mm'} \frac{f_{\mu m} f_{m\mu'} g_{\mu' m'} g_{m'\mu}}{\Gamma + i(E_\mu - E_{\mu'})/\hbar} \, , \qquad (1)$$

where $R(f,g)$ is the rate at which photons of polarization $\vec{e}$ are absorbed and photons of polarization $\vec{e}'$ are reemitted, $f_{\mu m} = (\mu \,|\, \vec{e} \cdot \vec{r} \,|\, m)$ is the matrix element connecting the excited state μ to the ground state m when dipole radiation with polarization $\vec{e}$ is absorbed by the atom, and $g_{m'\mu'} = (m' \,|\, \vec{e}' \cdot \vec{r}' \,|\, \mu')$ is the dipole matrix element connecting the excited state μ' to the ground state m' when a photon of polarization $\vec{e}'$ is reemitted. The quantity $\Gamma = \tau^{-1}$ is the radiative decay rate of the excited state and E_μ and $E_{\mu'}$ are the energies of the μ' and μ excited-state sublevels, respectively. For these S-state level crossings, the hfs splitting is much greater than $1/\tau$ and the linear Zeeman approximation gives an adequate description of the zero-field level-crossing signals. In the experiment we used circularly polarized $^2P_{1/2} \rightarrow {}^2S_{1/2}$ excitation and circularly analyzed $^2S_{1/2} \rightarrow {}^2P_{3/2}$ decay with 90° scattering in the plane perpendicular to the dc field. For these conditions, using the linear Zeeman approximation, and deleting the terms for which μ and μ' refer to different hyperfine levels of the excited state, we obtain [8-10]

$$R_{(\pm)(\pm)'} \propto 1 - k_1 (\pm)(\pm)' \cos\theta \cos\theta' - k_2 (\pm)(\pm)' \sin\theta \sin\theta' \times [\cos(\phi' - \phi) + y \sin(\phi' - \phi)]/(1+y^2) \, , \qquad (2)$$

where $k_1 = 0.25$, 0.17, 0 and $k_2 = 0.125$, 0.05, 0.25, respectively, for Ga, In, and Tl. The angles θ and ϕ refer to the azimuthal and polar angles of the propagation direction of the exciting (unprimed) and detected (primed) radiation in a spherical coordinate system with H along the z axis (as in Ref. 9). The symbols $(\pm)$ and $(\pm)'$ refer to the

sense of circular polarization of the exciting and detected radiation, and

$$y = g_J \mu_0 H\tau/(2I+1)\hbar ,$$

with $g_J = 2$ and $I = \frac{3}{2}$, $\frac{9}{2}$, $\frac{1}{2}$ for Ga, In, and Tl.[11]

For each element, level crossings in both $^2S_{1/2}$ state hyperfine levels are contributing to the k_2 term in Eq. (1). Since these two g_F values have equal magnitudes but opposite signs for each element, the two signals have the same form of field dependence but opposite signs. Thus the combined level-crossing signal in Eq. (2) is unambiguously related to τ, but owing to this partial cancellation it is not a very large percentage of the total fluorescence ($k_2 \ll 1$).

The average scattering angles[12] in the experiment were nominally $\langle\theta\rangle = \langle\theta'\rangle = \langle\phi' - \phi\rangle_{av} = \frac{1}{2}\pi$. We did not attain these exact angles so it is necessary to consider the $(\cos\langle\phi' - \phi\rangle_{av})/(1+y^2)$ term in Eq. (2) in the analysis of the results, although it is generally much smaller than the $y(\sin\langle\phi' - \phi\rangle_{av})/(1+y^2)$ term. Also, the circular polarizer and analyzer were not exact. This causes a decrease in k_1 and k_2 in Eq. (1) and potentially influences the ratio of the cosine and sine terms; but the relationship of τ to the measured field dependence is unaltered. The general form of Eq. (2) applied to the experiments is, thus,

$$\bar{R}_{(\pm)(\pm)'} \propto 1 - (\pm)(\pm)' k(\alpha + y)/(1+y^2) , \qquad (3)$$

where k was typically 75% of k_2 and $\alpha \ll 1$ represents the nonzero value of $\cos\langle\phi' - \phi\rangle_{av}$.

For the $^2S_{1/2} - {}^2P_{3/2}$ fluorescence, the Breit formula predicts a partial cancellation between the level-crossing signals due to excitation from the $n\,^2P_{1/2}$ and $n\,^2P_{3/2}$ states. For each excitation channel there is a similar cancellation between the signals arising from the $^2S_{1/2}$ to $^2P_{1/2}$ and the $^2S_{1/2}$ to $^2P_{3/2}$ fluorescence. However, both modes of excitation and decay produce the same form of magnetic field dependence so there is no complication in interpreting the signal when both modes of excitation and decay are present in the observed signal. In these experiments, optical filtering transmitted primarily the $^2P_{1/2} - {}^2S_{1/2}$ line for excitation and the $^2S_{1/2} - {}^2P_{3/2}$ line from the fluorescence, but no special care was taken to prevent small percentage leakages of the other lines.

The small addition of a symmetric level-crossing signal due to $\alpha \neq 0$ causes little difficulty as long as $\alpha \ll 1$ (α was normally less than 0.1 in these experiments). The signals were obtained by lock-in detection with small amplitude field modulation, so that they had the approximate form

$$\frac{d\bar{R}}{dH} \propto \frac{1 - 2\alpha y - y^2}{(1+y^2)^2} .$$

The asymmetry in these signals, due to the α term, is apparent in the positions of the nulls which occur at $y \cong \pm(1 + \frac{1}{2}\alpha^2) - \alpha$. This asymmetry, which is first order in α, was used to obtain α for each set of data. The width between the nulls changes only by $\frac{1}{2}\alpha^2$ and is easily corrected.

A. Departures from "White-Light" Approximation

The Breit formula is applicable when the exciting radiation has a constant power density at all frequencies which can induce a transition from the components of the ground state to those of the excited state. In these experiments departures from this "white-light" condition could arise from two sources: (i) The frequency spectrum of the exciting radiation may be significantly altered by absorption as it passes through the scattering vapor; and (ii) the lamp power spectrum is generally not flat across the absorption profile of the vapor. The magnetic scanning of these two types of nonwhite power spectrums by the field-dependent absorption profile of the vapor will be referred to as beam-absorption scanning[13] (BAS) and lamp-spectrum scanning (LSS). These two effects are distinguishable by their different dependence on beam density. The field-dependent variation of fluorescence intensity due to the LSS is a constant proportion of the fluorescence since it results from the optically thin beam magnetically scanning the lamp profile. The BAS results from the scanning by beam atoms further from the lamp of a spectral absorption feature produced by the atoms nearer the lamp. The size of this absorption feature is proportional to beam density, so the BAS is a varying proportion of the total fluorescence. For low-beam optical depths the size of the LSS varies linearly with beam density, while the BAS varies quadratically. To elaborate on the appropriateness of "low optical depth" in these discussions, we note that the LSS and BAS could distort our Hanle-effect signals by several percent at beam densities which absorbed less than 0.1% of the lamp resonance lines; this was typical of the beam densities used in the experiments. The method of correcting the data for these effects is based on the following arguments.

Gallagher and Lurio[14] have given the following expression for the average fluorescence from a vapor of atoms, with a velocity distribution $n(V_x)$, excited by light possessing an arbitrary power-density spectrum $\rho(\nu)$:

$$R(\bar{f},\bar{g}) = C' \sum_{\substack{\mu,\mu' \\ m,m'}} \frac{f_{\mu m} f_{m\mu'} g_{\mu' m'} g_{m'\mu}}{\Gamma + i\omega_{\mu\mu'}} \times 8\pi \int_{-\infty}^{\infty} d\nu \int_{-\infty}^{\infty} dV_x\, n(V_x)\rho\left(\nu - \frac{V_x \nu}{c}\right) \times \left(\frac{1}{\nu - \omega_{\mu m} + \frac{1}{2}i\Gamma} - \frac{1}{\nu - \omega_{\mu' m} - \frac{1}{2}i\Gamma}\right) . \qquad (4)$$

Since $\rho(\nu)$ was not measured in these experiments, Eq. (4) cannot be used to calculate the expected signal shapes. However, the field dependence of the fluorescent intensity was measured without polarizers to detect the scanning of the beam-absorption profiles across the exciting spectrum in the absence of the Hanle-effect signals. This corresponds to detecting the field dependence of the "diagonal" ($\mu = \mu'$) terms in Eq. (4).[15] When the fluorescence is then analyzed for circular polarization to observe the Hanle-effect signals arising from the $\mu \neq \mu'$ terms, the sum of the $\mu = \mu'$ elements produces the

$$1 - k_1(\pm)(\pm)' \cos\theta \cos\theta'$$

terms in Eq. (2). The 1 arises from the same sum of the diagonal elements in Eq. (3) that occurs when the fluorescence is not analyzed, so its field dependence (due to nonwhite light) is precisely what is measured with the fluorescence analyzer removed. The field dependence of this leading term can thus be accurately removed from the Hanle-effect signals. The k_1 term in Eq. (2) is nominally zero for our average scattering angles, and the field dependence of any residual portion is quite negligible. It can be seen from Eq. (4) that Hanle-effect signals, which come from $\mu \neq \mu'$ terms, will have more than just the $[\Gamma + i\omega_{\mu\mu'}(H)]^{-1}$ field dependence which led to the $y(1+y^2)$ dependence in the k_2 term of Eq. (2). However, the percentage distortion of these terms due to the nonwhite light will be similar to the percentage distortion of the much larger leading term. Thus, from our measurements on the leading term (scattering unpolarized light) we could infer that the distortion of the Hanle-effect signal terms was negligible under the experimental conditions. Essentially, the nonwhite spectrum causes a quite small percentage variation with field; it is only important in the diagonal terms because the Hanle-effect size (k_2) is also a small percentage of those terms.

Using this approximation to analyze the measurements, we replace the 1 in Eq. (3) by $1 - \epsilon(H)$, where $\epsilon(H) \ll 1$ was measured in the unpolarized scattering experiment (the unpolarized light signals were attenuated with neutral density filters to yield the same total fluorescence at zero field as with polarizers in),

$$R_{(\pm)(\pm)'} \propto 1 - \epsilon(H) + (\pm)(\pm)' k(\alpha + y)/(1 + y^2) \quad . \qquad (5)$$

To support the validity of using Eq. (5) to analyze the signals, the field dependences for unpolarized scattered light were compared to $\frac{1}{2}(R_{++} + R_{-+})$. According to Eq. (5) the resulting lock-in signals should be the derivative of $\epsilon(H)$ in both cases. While the unpolarized signal varied from 0 to 30% of the peak Hanle-effect signal, the comparison always agreed within the experimental uncertainty that varied from 0.3 to 2% of the peak Hanle-effect signals.

One other aspect of these nonwhite light effects should be noted. The $\epsilon(H)$ term caused only a few percent distortions of the Tl Hanle-effect signals, larger distortions (up to 5%) for Ga, and quite large distortions (up to 30%) for In. This is partly a result of the k_2 values ($\frac{1}{4}$, $\frac{1}{8}$, $\frac{1}{20}$ for Tl, Ga, In) and partly a consequence of the g_F (1, $\frac{1}{2}$, $\frac{1}{5}$ for Tl, Ga, In). The importance of g_F follows from the fact that the $\Delta m = 1$ level crossings are between adjacent levels whose separation is $g_F \mu_B H$, whereas the scanning of the exciting spectrum occurs between different F and m levels of the $^2S_{1/2}$ and $^2P_{1/2}$ states. On the average, the variation of such level separations is about $2\mu_B H$.

B. Form of Signal Resulting from Modulation and Phase Sensitive Detection

In order to reduce the noise resulting from drifts in the lamp intensity and beam density, the fluorescence signal was modulated by adding a sinusoidally varying field $\hat{z} H_\omega \cos\omega t$ to the static field $\hat{z} H$. The photomultiplier signal was amplified and phase sensitive detected at frequency ω. The signal obtained by this procedure is the coefficient of $\cos\omega t$ in the Fourier expansion of $R(y + y_\omega \cos\omega t)$, where $R(y)$ is given by Eq. (5),

$$y_\omega = 2H_\omega / H_{1/2}, \; y = 2H/H_{1/2},$$

$$H_{1/2} = 2(2I+1)\hbar / g_J \mu_B \tau \; .$$

In these experiments y_ω was generally less than 0.4 so that $R(y + y_\omega \cos\omega t)$ can be evaluated by means of a power series expansion [$\epsilon(y)$ has a characteristic width greater than $\frac{1}{2}H_{1/2}$]. The first three terms of the expansion were used to fit the experimental data:

$$S \cong \left(y_\omega \frac{d}{dy} + \frac{1}{8} y_\omega^3 \frac{d^3}{dy^3} + \frac{1}{192} y_\omega^5 \frac{d^5}{dy^5} \right) R(y) \quad . \qquad (6)$$

This expression is accurate to better than 0.4% of its maximum value even when $y_\omega = 0.7$. The measurements have been analyzed in terms of Eq. (5) in Eq. (6); the fundamental problem is determining in each of these experiments the value of $H = \frac{1}{2}H_{1/2}$ for which $y = 1$.

III. APPARATUS

The basic apparatus and scattering geometry were the same for each experiment. A diagram of this apparatus is shown in Fig. 1. Circularly polarized resonance radiation excited the atomic beam and circularly polarized fluorescence was detected; the optical axes were in the horizontal plane with the beam directed upwards.

The oven consisted of a carbon crucible and stainless-steel heat shield surrounding a spiral

tungsten heater; alumina rods supported these parts. The oven operated at temperatures of 400–500 °C for Tl and 700–900 °C for Ga and In. The magnetic fields in the scattering region due to the heater current were less than 0.1% of the Hanle-effect linewidths and thereby negligible in these experiments. The background gas pressure was always below 10^{-6} Torr when data were being taken.

The atomic-beam collimation partly determined the absorption spectrum of the beam. A 1-in.-diam hole 2.8 in. above the $\frac{3}{8}$-in.-diam source aperture in the heat shield and 2 in. below the center of the scattering region collimated the beam. The beam was collected on a liquid air-cooled surface to decrease occasional bounces onto the windows. In the scattering region the beam was approximately 1.75 in. diameter, which was about twice the diameter of the incident radiation cone.

The resonance lamps used in the thallium and gallium experiments were Phillips resonance lamps (the fluorescing area was $\sim\frac{1}{2}\times 1$ in.). For the indium experiment two types of lamps were used, a Phillips indium resonance lamp and an electrodeless indium-iodide resonance lamp (also $\sim\frac{1}{2}\times 1$ in.). The indium-iodide resonance lamp was made by heating chips of indium and iodine in a partially evacuated 12-mm quartz tube, then evacuating all of the excess iodine, backfilling with about 2 Torr of argon, and sealing off the tube. It was operated with the top of the tube directly under a 2.45-GHz diathermy "A head." The indium-iodide vapor pressure was contolled with heating tape wound around the remainder of the tube. The Phillips lamps were driven by a Phillips power supply, which was run from a Variac to vary the driving power.

The lenses and their relative locations in the experiment can be seen from Fig. 1. The lamp optics were arranged so that the lens closest to the lamp illuminated the second lens, which in turn imaged the first lens onto a plane in the center of the interaction region.

The detection optics imaged the entire beam onto the 2-in. photocathode with a magnification of about 1. The circular polarizer and analyzer used mica plates ~1 mil in thickness, corresponding to $\sim\frac{1}{4}\lambda$ retardation. These had some "patches" of slightly varied thickness, but this only influenced the values of R and α in Eq. (5) so it was not considered important.

Interference filters of ~50-Å half-width were used to transmit the Ga 4033- and 4172-Å lines and the In 4102-Å line. Glass absorption filters were used for the In 4511-Å line and the Tl 3776-Å and 5350-Å lines. The photomultiplier was an RCA 5819 operated at 700–1100 V. The photomultiplier and lamp were located in a fringing field of the Helmholtz coils that was ~5% of the field in the scattering region. The photomultiplier was shielded by Mumetal but its output still increased by 0.1% at 80 G and 0.5% at 130 G. The Phillips lamps did not display measureable field dependence, but the indium-iodide lamp varied a small fraction of 1% even with some shielding. These minor field dependences acted only as scale factors for the lock-in signal size, since the fringing field of the smaller modulation coils was much smaller at the lamp and photomultiplier. Since the lock-in signals were very small at such large fields, this was a negligible distortion.

The static field was calibrated in the scattering region in terms of the potential across a precision series resistor: The calibration fields were measured with a rubidium magnetometer. A $\pm\frac{1}{2}$% uncertainty was assigned to this calibration. The field was homogeneous within 0.2% throughout the 1.75-in.-diameter, 1-in. high scattering region.

The modulation field $\hat{z}H_\omega \cos 2\pi ft (f = 37\,\mathrm{Hz})$ was also calibrated with a Hall gaussmeter using a dc

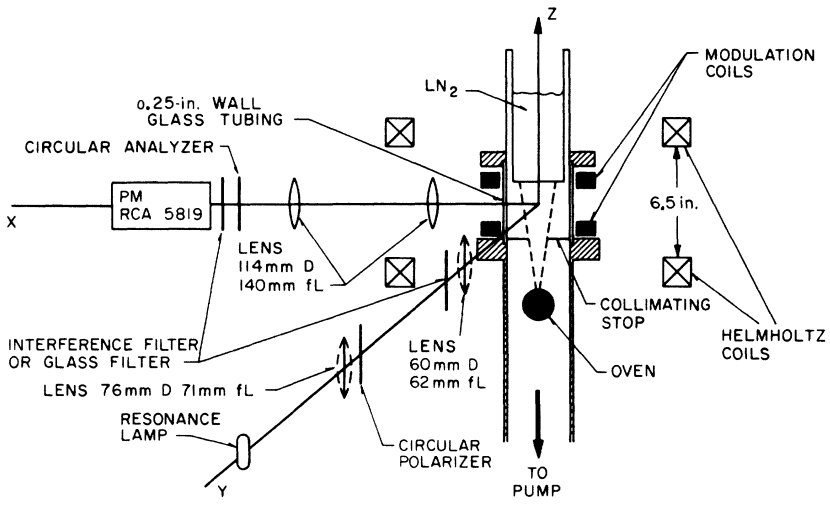

FIG. 1. Diagram of apparatus with X-Z plane to scale.

current. In the experiments no attempt was made to cancel the earth's magnetic field of ~0.4 G along H and ~0.3 G transverse since the parallel component merely causes a scale shift and the transverse component has a negligible effect on these Hanle-effect signals with 15-, 33-, and 82-G linewidths.

Instabilities in the lamp intensity and atomic-beam density were some of the major sources of noise in the experiments. Since the Hanle-effect signals were a small percentage of the total scattering, field modulation and phase sensitive detection were used to reduce, relative to the signal, the noise resulting from these instabilities. The output of the photomultiplier was filtered by a preamplifier with a 120-cps notch filter to prevent saturating the amplifiers of the lock-in with the 120-cps modulation which resulted from the lamps being driven at 60 cps. The total output current of the photomultiplier was also recorded to monitor the fluorescent intensity. Measurements of relative beam densities (for a given experiment) were then obtained from a knowledge of the resonance fluorescence at $H=0$ and the lamp intensity as monitored by a photodiode. (Variations of lamp profile disallow this as an accurate monitor of beam density, but it provides useful relative information.)

IV. MEASUREMENTS AND RESULTS

As noted above, the effect of small but nonzero α in Eq. (5) (asymmetry) could be accurately corrected for since it appears as a first-order asymmetry in the signals but it increases the width only by the factor $1+\frac{1}{2}\alpha^2$. In the ensuing discussions all widths have been corrected in this manner for measured asymmetries.

To obtain optimum signal-to-noise ratios S/N but only minor signal distortions, most of the data were taken at modulation fields corresponding to $y_\omega \simeq 0.3$. The modulation broadening was then separately evaluated for each element by measuring the linewidths as a function of H_ω. (All conditions other than modulation amplitude were fixed during each of these broadening measurements.) The widths should be compared to Eq. (5) in Eq. (6), but ϵ in Eq. (5) was so small that it could be ignored in all but the $y_\omega d/dy$ term of Eq. (6). A computer calculation confirmed that the other terms, as well as the higher derivatives of the α term, are almost undetectable at the experimental conditions. Indeed, the computed broadening never differed by more than a small fraction of 1% from $1+\frac{3}{8}y_\omega^2$, which arises from just the first two terms of Eq. (6) operating on $R(y)\propto 1-y/(1+y^2)$. Consequently the linewidth data were plotted against V_ω^2 ($\propto y_\omega^2$) in the standard fashion and a straight line was fitted to obtain the unbroadened width (see Fig. 2). The slope of this line and the value of $\frac{1}{2}H_{1/2}$ determined by the extrapolation were then used in conjunction with the relationship

$$H_{1/2}(H_\omega) = H_{1/2}[1+\tfrac{3}{2}(H_\omega/H_{1/2})^2]$$

to obtain the calibration of H_ω in terms of the modulation voltage V_ω. These calculations of H_ω (at 37 Hz) give 15.5 ± 1.2, 15.4 ± 0.8, and 15.2 ± 0.6 G/V from the Ga, In, and Tl data. (The current was recorded in terms of the voltage across a series resistor.) The dc gaussmeter calibration described in the Sec. III gave 15.9 G/V at the center of the modulation coils. Since the modulation-broadening calibrations represent the average modulation field over the scattering volume, slightly lower fields are expected. This excellent agreement on modulation-field amplitude supports the assignment of quite small percentage uncertainties

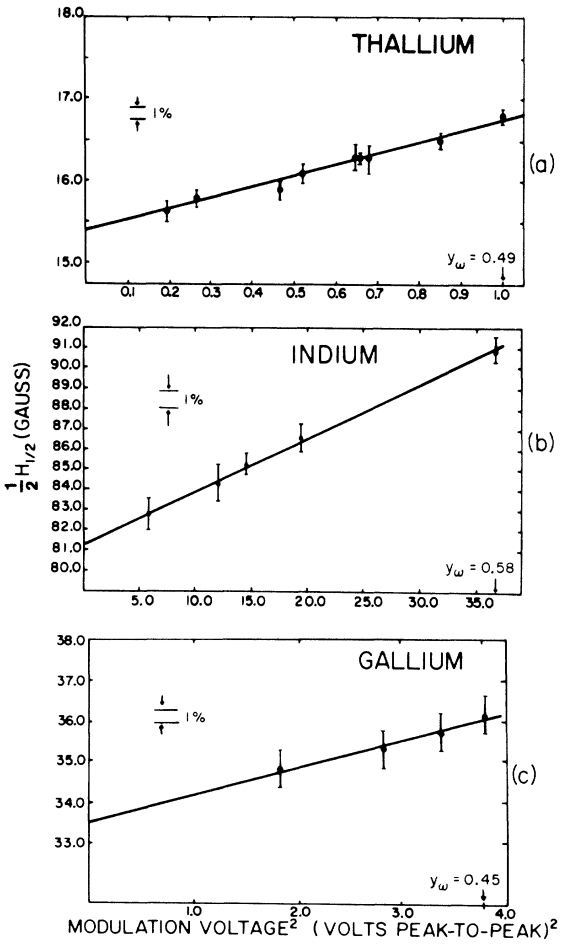

FIG. 2. Modulation-broadening data. The best straight-line fits to the data are indicated. These data were taken at beam densities (in the fluorescent intensity units of Figs. 5 and 6) of 2 for Tl, 1 for In, and 0.4 for Ga. V_ω, the voltage across a resistor in series with the modulation coils, is proportional to H_ω.

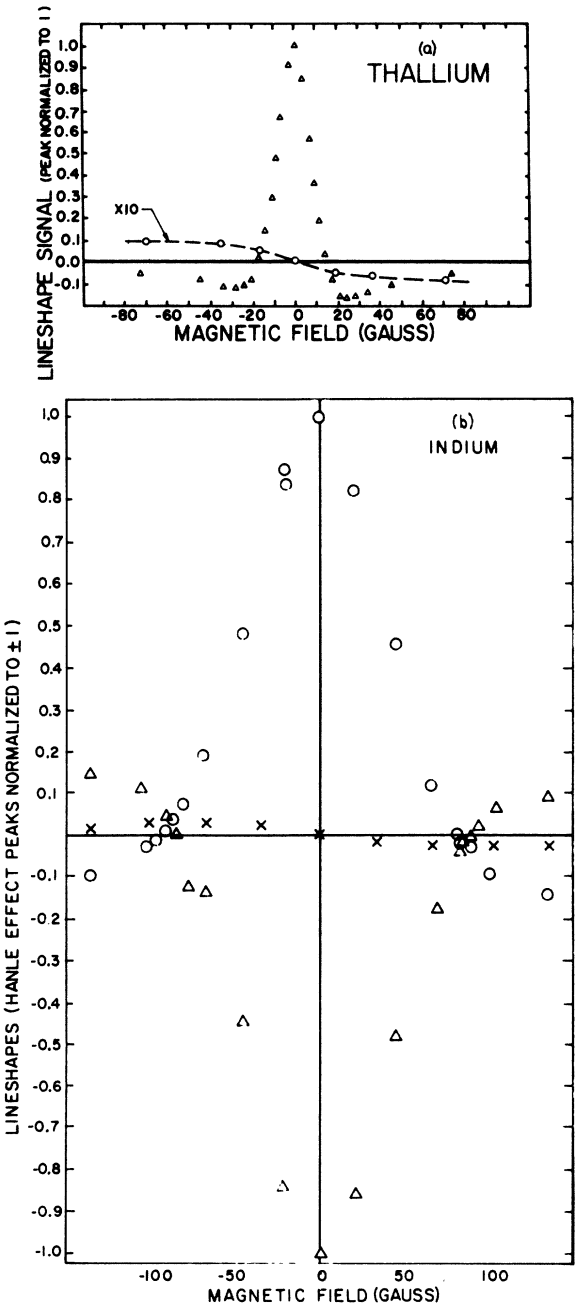

FIG. 3. (a) Uncorrected thallium Hanle-effect signal normalized to 1 at the peak (Δ) and unpolarized fluorescence signal (o) for the same total intensity at $H=0$. The asymmetry coefficient $\alpha = 0.07$. (b) Indium signals, normalized to 1 at the peak. The detected fluorescence was circularly analyzed while the incident was positive circular (o), negative circular (Δ), and unpolarized (×).

to the various modulation-broadening corrections.

For each element, the LSS and BAS contributions to the signals were measured by replacing the circular polarizer with a neutral density filter, of a density that gave the same resonance fluorescence intensity at $H=0$ as the circular polarizer. This neutral density signal was subtracted from the circularly polarized fluorescence signal to establish the correct $H_{1/2}$ in the approximation of Eqs (5) and (6). For most of these width data, measurements were taken only at $H=0$ and in the neighborhood of $y=\pm 1/\sqrt{3}$, where the nulls of the corrected signal occur. Both senses of circular polarization were used when the neutral density signals were greater than a few percent of the peak Hanle-effect signals; within experimental error the same nulls were always obtained. {The LSS and BAS signals have the opposite symmetry of the Hanle-effect signals, so they produce primarily a shift of the nulls with minor broadening. Without corrections, the shifts are in opposite directions for opposite sense of incident circular polarization [see Eq. (5)].} Examples of the actual signal shapes are given in Fig. 3.

To support the validity of the corrections, and to search for indications of systematic error, data with both senses of incident circular polarization were taken over a range of fields. After subtraction of the unpolarized scattering signals, these data were compared to Eqs. (5) and (6) with $\epsilon = 0$. The measured and theoretical signals were normalized to unity at $H=0$, H_ω was determined from V_ω and the above calibration, and α and $\frac{1}{2}H_{1/2}$ were chosen so that the nulls of the theoretical and experimental data coincided. Plots of the difference between these theoretical and experimental lock-in signals will be referred to as "theory minus experiment." In assigning probable errors to the measured lifetimes these residuals were regarded as an indication of the possible size of effects which had not been accounted for in the experiments, although the scatter could have been produced entirely by photomultiplier noise and drifts. Plots of these residuals are given in Fig. 4.

To check for possible coherence narrowing, width measurements were made with H_ω constant at a variety of beam densities. The width at each density was found after correcting for LSS and BAS and asymmetry. These data are presented below in Secs. IV A–IV C.

A. Thallium

The thallium 7 $^2S_{1/2}$ lifetime had already been measured by zero-field level-crossing techniques,[14] but it was repeated in this set of experiments because it produced the largest Hanle-effect signal of the three elements and was thus more easily analyzed for systematic errors which might have been present. In addition, this measurement allowed us to check our results against another Hanle-effect experiment.

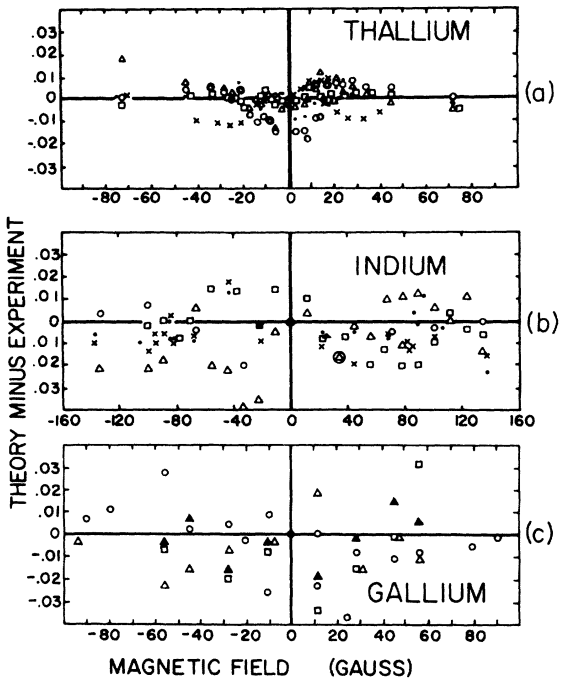

FIG. 4. Theory-minus-experiment residuals on a scale of 1.0 for the peak Hanle-effect signals. Data for each element include runs with opposite senses of exciting circular polarization and with different asymmetry coefficients. Modulation voltages (see Fig. 2) were 0.68, 3.7, and 1.4–1.9 V for Tl, In, and Ga, respectively. The beam densities, in the fluorescent intensity units of Figs. 5 and 6, were 2.6, 0.5–0.8, and 0.4 for Tl, In, and Ga, respectively.

The major sources of noise in these data were drifts in lamp intensity and atomic-beam density. Drifts of 1–2% in the resonance fluorescence intensity would occur in the course of an hour, the time required to take a full line shape.

The presence of a small contribution from a BAS effect was found when a neutral-density filter was used to replace the circular polarizer. The typical size and shape of this signal compared to the corresponding Hanle-effect data (for clockwise-circular polarization) is shown in Fig. 3(a). A plot of the ratio of this BAS + LSS signal/peak Hanle effect as a function of beam density is shown in Fig. 5(a). These data fit a straight line, indicating that the size of the signal was proportional to the square of the beam density. From this we concluded that the signal obtained with the neutral-density filter is largely due to the BAS. For thallium, this BAS signal caused such small distortions that correcting for it caused at most a 1% correction to the linewidth. The absence of a LSS was not unreasonable since the natural linewidth is 21 MHz, while the characteristic width of the lamp radiation is greater than the 600 °C Doppler width of 1200 MHz. Also $g_F = 1$ for the Tl $^2S_{1/2}$ state, so the spectral scanning is not much faster than the $\Delta m = 1$ level crossings (see discussion in Sec. II).

From the measurements of modulation broadening a value of $\frac{1}{2}H_{1/2} = 15.4 \pm 0.15$ G was obtained, where the widths were corrected for BAS and asymmetry [Fig. 2(a)].

In Fig. 4(a) we can see the "theory-minus-experiment" data for thallium, which represent five different "line-shape determinations." From these data we conclude that any line-shape errors contributed less than 1% uncertainty to the measured $\frac{1}{2}H_{1/2}$. This represents our best test for a variety of possible systematic errors. Using Eqs. (5) and (6) and the V_ω calibration to fit these line shapes, $\frac{1}{2}H_{1/2}$ values of 15.2, 15.3, 15.4, 15.1, and 15.2 G are obtained.

The measurements of the dependence of $\frac{1}{2}H_{1/2}(H_\omega)$ on beam density are shown in Fig. 6(a). As can be seen these measurements were made for two different modulation voltages. Each of these sets of measurements appears to fit a constant width although the $V_\omega^2 = 0.5V^2$ data give a width in Fig. 2(a) that is only in marginal agreement with the other data. It was concluded that the uncertainty in the extrapolation of $\frac{1}{2}H_{1/2}$ to zero density was less than 0.5%.

Our final determination of $\frac{1}{2}H_{1/2}$ (15.3 G) was the average of the value from the modulation-broadening data combined with the average value determined from the theory-minus-experiment data. The estimated error in this measurement results from ±1.0% uncertainty in our determination of $\frac{1}{2}H_{1/2}$, ±0.5% uncertainty in our calibration of the magnetic field, 0.5% uncertainty due to coherence narrowing, and ±1.0% uncertainty due to possible additional systematic errors. Taking *the sum of the above errors as our estimate of the maximum probable error in the measurement* of the thallium $7\,^2S_{1/2}$ lifetime, we conclude that the lifetime is $(7.45 \pm 0.2) \times 10^{-9}$ sec.

B. Indium

Two different lamps were used in the experiment, a (Phillips) indium resonance lamp and an electrodeless InI_3 lamp of our own construction. Unlike thallium, both indium lamp intensities had a significant wavelength dependence. A significant BAS was also present in the data. Figure 5(c) shows BAS + LSS line shapes which were obtained with a neutral-density filter replacing the circular polarizer. The maximum to minimum sizes of the BAS + LSS signals were divided by the peak Hanle-effect signals and plotted as a function of fluorescent intensity in Fig. 5(b). The fact that the data in Fig. 5(b) do not extrapolate to zero at zero beam density is taken as evidence for the presence of a LSS effect while the slope is attri-

buted to BAS. Other data in which the beam conditions were unchanged but the lamp conditions varied were also taken; these data showed a change in the field dependence of these signals as the lamp conditions were varied, which also indicated the presence of a LSS. (The corrections of the Hanle-effect data do not depend on this distinction between LSS and BAS effects.)

The S/N in the indium measurements was much smaller than it was for thallium. This was partly a result of the Hanle-effect signal being a much smaller proportion of the total resonance fluorescence [Eq. (2)] and partly from the necessity of keeping the beam density much smaller for In to avoid excessive signal distortions. The major sources of noise, however, were instabilities in the lamp conditions which caused the LSS and total intensity to vary.

As an indication of optical depths in the beam, it is interesting to note that at the maximum beam densities in Fig. 5(b), a photodiode monitoring the transmitted lamp intensity increased $\frac{1}{2}\%$ when the beam flag was closed. Noting that the radiation and beam angles caused the beam to absorb over about $\frac{1}{3}$ of a Doppler width, while the expected lamp linewidth is a few Doppler widths, this corresponds to a beam optical depth in the neighborhood of 0.04.

The data in Fig. 6(b) show the variation of $\frac{1}{2}H_{1/2}(H_\omega)$ with beam density. As indicated by the fitted line, these data are consistent with about 2% coherence narrowing at the maximum densities. Since the modulation-broadening and line-shape data were taken at beam densities between 20 and 40% of this maximum, they will be corrected by $+0.5\pm0.5\%$ to account for the apparent narrowing indicated by Fig. 6(b).

The "theory-minus-experiment" data given in

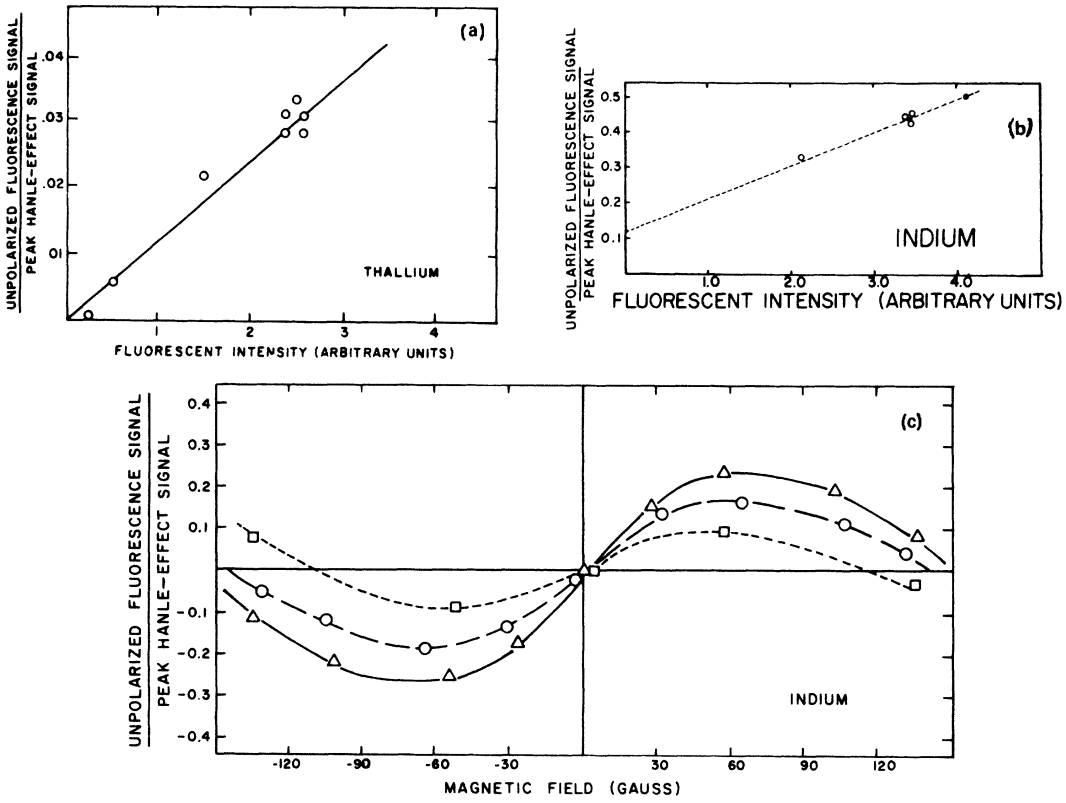

FIG. 5. (a) and (b) BAS + LSS signals/peak Hanle-effect signals as a function of beam density. (Beam density is proportional to fluorescent intensity.) These data were taken with a neutral-density filter replacing the circular polarizer to give the same intensity of fluorescence at $H=0$. The beam scan signal is the distance between its maximum and minimum values (see Fig. 3). The lines are for purposes of comparison only; the indium intercept at zero fluorescence is attributed to LSS; the slopes are attributed to BAS. This separation is made for interpretive interest only; the analysis of the Hanle-effect data did not depend on separating the LSS and BAS effects. (c) Indium line-shape signals taken with unpolarized exciting light. The lamp conditions were the same for all of these data, but the beam densities (which are proportional to fluorescent intensity), were varied. See Fig. 6 for units of fluorescent intensity. □ denotes 2.2 units of fluorescent intensity; o denotes 3.4 units of fluorescent intensity; Δ denotes 4.1 units of fluorescent intensity.

Fig. 5(b) were obtained for five different conditions. The values of $\frac{1}{2}H_{1/2}$ that best fitted these data with Eqs. (5) and (6) were 81.3, 81.9, 81.4, 80.8, 83.0 83.0 G. From the residuals in Fig. 5(b), we surmise that any residual line-shape error was less than 2%.

The value of $\frac{1}{2}H_{1/2}$ determined from the $\frac{1}{2}H_{1/2}(H_\omega)$-vs-$V_\omega^2$ data was 81.3 G; the average value of $\frac{1}{2}H_{1/2}$ determined from the "theory-minus-experiment" data was 81.7 G. Averaging these values and adjusting by +0.5% for coherence narrowing gives $\frac{1}{2}H_{1/2}$ = 81.9 G. We estimate uncertainties of ±0.5% from coherence narrowing, ±½% from the field calibration, ±1% from random fluctuations in the measurements, and ±2.0% from possible systematic errors indicated by the "theory-minus-experiment" residuals. *Taking the sum of these errors* to be the maximum uncertainty in our measurement of $\frac{1}{2}H_{1/2}$ we conclude that the lifetime of the $6\,^2S_{1/2}$ state of indium is $(7.0 \pm 0.3) \times 10^{-9}$ sec.

C. Gallium

The major source of noise in this experiment was drifts in the lamp intensity and atomic-beam density. These drifts caused 1–3% uncertainties in some of our measurements of the signal shape, but the width measurements were largely independent of the drifts. Since Ga required the highest oven temperatures, we operated at considerably lower beam densities than in the Tl and In cases.

No contribution to the signal from LSS or BAS was seen in this experiment (within typical experimental uncertainties of 1%). Also, less than 0.1% change in the output of a photodiode monitoring the lamp intensity was seen as the beam flag was opened and closed, which was in agreement with the absence of any BAS as well as the absence of coherence narrowing.

The plot of the $\frac{1}{2}H_{1/2}(H_\omega)$-vs-$V_\omega^2$ data is shown in Fig. 2(c). The data in Fig. 6(c) show the dependence of $\frac{1}{2}H_{1/2}$ on beam density. From these data we conclude that any error introduced by not correcting the data for coherence narrowing is less than 0.5%.

The "theory-minus-experiment" data in Fig. 4(c) are the result of four different line shapes. The following four values of $\frac{1}{2}H_{1/2}$ were used in fitting these line shapes: 33.6, 34.0, 33.8, and 33.8 G. As can be seen, the data obtained indicate a great deal of "scatter." This scatter was believed to be due to drifts in the beam and lamp conditions, but because of this scatter it appears that undetected line-shape errors could be as large as ±3%. On the other hand, the In and Tl data and the internal consistency of the Ga data make this very unlikely. The extrapolation of the modulation-broadened data in Fig. 2(c) gives

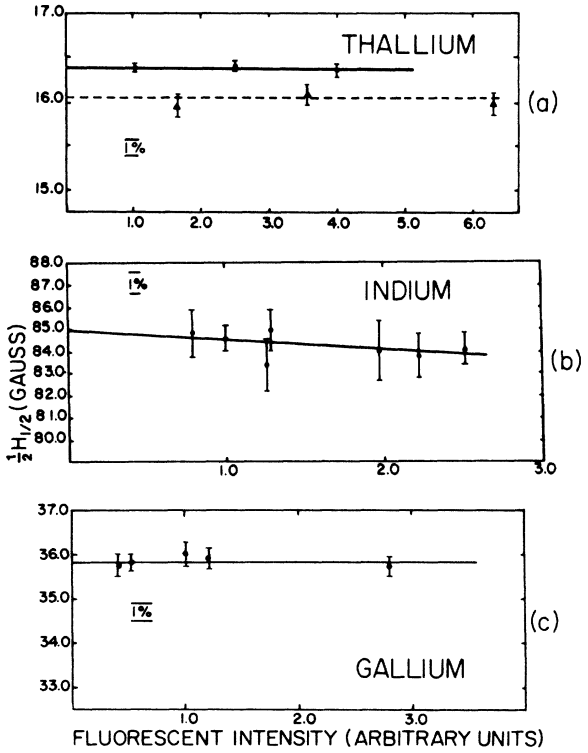

FIG. 6. Dependence of $\frac{1}{2}H_{1/2}(H_\omega)$ on beam density (beam density in units of fluorescent intensity). The data were taken at modulation voltages of 0.68–0.81 V for Tl, 3.5 V for In, and 1.84 V for Ga. The straight-line fits correspond to no coherence narrowing for Tl and Ga, and 1–2% narrowing for In. The small percentage Hanle-effect signals for indium required higher beam densities in that case.

$\frac{1}{2}H_{1/2}$ = 33.6 G; the average of the line-shape data fits in Fig. 4(c) gives 33.8 G. We estimate uncertainties of ±1% due to random fluctuations in the data from which $\frac{1}{2}H_{1/2}$ was determined, ±½% due to the magnet calibration, ±2% error due to possible systematic effects, and ±0.5% due to coherence narrowing. Taking *the sum of these as the maximum error*, we obtain $(6.8 \pm 0.3) \times 10^{-9}$ sec for the gallium $5\,^2S_{1/2}$-state lifetime.

V. DISCUSSION

A review of prior measurements of the lifetimes reported here is included in Ref. 5. We have relisted these measured lifetimes in Table I for comparison with the present results. The atomic-beam-absorption method utilized a microbalance measurement of atomic-beam density, and the hook measurements used vapor-pressure data to establish the lifetimes from the measurements. The remaining measurements, by phase-shift or Hanle-effect techniques, all measure the lifetimes directly and should be more accurate. Yet a glance at Table I (and the footnote) will confirm that only

TABLE I. Experimental lifetimes.

Measurement	Ga $5\,^2S_{1/2}$ (nsec)	In $6\,^2S_{1/2}$ (nsec)	Tl $7\,^2S_{1/2}$ (nsec)
Present work (Hanle effect)	6.8±0.3	7.0±0.3	7.45±0.2
Double resonance and Hanle effect (Ref. 14)	...	...	7.6±0.2
Phase shift (Ref. 5)	7.6±0.4	7.5±0.3	7.65±0.2
Phase shift (Ref. 4)	...	8.5±0.1	...
Phase shift (Ref. 16)	9.9±0.2	...	8.7±.3[a]
Atomic-beam absorption (Ref. 17)	11.4±1.7	8.35±1.2	8.1±0.8
Hook (Ref. 18)	6.4±2.4	6.3±0.8	8.25±0.6

[a]Cunningham and Link (Ref. 5) note a private communication from Dr. Demtröder, who had remeasured this lifetime and found agreement with their value.

the Tl measurements agree within the assigned errors. The agreements for Ga and In are good compared to the uncertainties that existed several years ago, but they clearly indicate unevaluated systematic error in some or all of the experiments.

Reference 16 represents the results of the pioneering work by the phase-shift technique. As is to be expected, time and S/N considerations precluded careful measurements of phenomena that were more easily studied in the succeeding work of Refs. 4 and 5. Indeed it is noted in Ref. 5 that Demtröder has since made another evaluation of the Tl lifetime and found agreement with Ref. 5; on the basis of the variety of problems noted in Refs. 4 and 5 and below, we will assume that Demtröder's Ga result is also subject to revision.

The results reported in Refs. 4 and 5 and the present work are within a 20% bracket for In and 12% for Ga even though the estimated errors do not overlap. The discrepancies are as great between the different phase-shift measurements as between them and our Hanle-effect results. It is interesting to note that an earlier measurement by Link agreed quite well with Hanle-effect and other measurements for alkalis.[3] Similarly, Ref. 4 included lifetimes of alkaline earths that are in very good agreement with Hanle-effect measurements. We have discussed above all the sources of systematic error that were considered in the present experiments, and the method of assigning uncertainty to them. To balance this, it appears appropriate to now discuss some of the sources of systematic errors that can affect phase-shift experiments.

The phase-shift technique is essentially a measurement of the time delay between exciting and fluorescent radiation. An extrapolation of the measured delay to zero density of fluorescing atoms is clearly necessary to correct for radiation trapping. Such extrapolations, complicated by a correction for a wall-scattered component of the fluorescence, were carried out in Refs. 4 and 5, although the data from which the Ga and In extrapolations were made were not presented. It appears reasonable to assume that errors can arise if S/N is inadequate to allow a good extrapolation.

Because of the characteristics of the light modulators used, it was essential to average correctly over the exciting light beam to obtain the "zero phase" for instantaneous scattering. Since different components of the incident light beam had phase variations of ~10°, or 5 nsec for 5 Mc modulation, it was necessary to average over these components in exactly the same manner with the instantaneous scattering object as with the fluorescing atomic beam.[4,5] Since the fluorescing region was in vacuum, this was not a simple operation. In Ref. 5 the time of flight of photoelectrons in the photomultiplier was also found to vary by 1–3 nsec with wavelength and position on the photocathode.

In addition to these major effects, which were discussed and presumably allowed for in Refs. 4 and 5, a number of second-order effects that were not considered could also affect the results. We list four examples: (a) The variation of atomic-beam optical depth with incident radiation angle can cause varying attenuation of different angular components of the incident light (whose phases differ). (b) Any variation in the optical line profile across the lamp could result in different average phases for different parts of the incident spectrum. The instantaneous scatterer does not distinguish between such components, but the atomic beam will. (c) The atoms at different parts of the atomic beam absorb light of different wavelengths due to their motion, and with the optics used in the experiments these different parts of the beam illuminated different parts of the photocathode. The intensity from the resonance lamps will vary with wavelength so that these different positions in the beam will be effectively illuminated by different intensities. Thus the beam will not fluoresce from the same average position as a scattering sol, and the variable time delay from different parts of the cathode may be differently averaged over (this potential error could be eliminated by imaging an objective lens onto the photocathode). (d) The optical modulator produces large components of modulated light at the rf harmonics and the atomic fluorescence phase-shifts these by more than the fundamental. Such anomalously large phase shifts will not affect the results only if the frequency-shifted oscillator has less than ~40-dB harmonic content.

The sizes of the effects discussed above cannot be reliably estimated and they may have been negligible in the experiments of Refs. 4 and 5. We note them to indicate that the phase-shift experi-

ments are also subject to a variety of possible systematic effects that could vary considerably between elements. We suggest that the very thorough investigation of systematic effects presented here makes our results more reliable, but this is certainly subject to revision if new factors come to light.

APPENDIX: CONTRIBUTIONS OF NONLINEAR ZEEMAN TERMS AND OF HIGH-FIELD LEVEL-CROSSING TERMS

Equation (2) was calculated from the Breit formula with the aid of two assumptions – that the Zeeman splitting was linear, and that the contributions were negligible from the terms in Eq. (1) with μ and μ' corresponding to states with $F \neq F'$.

Considering first the $F \neq F'$ terms, these have "*ffgg*" coefficients in Eq. (1) that are of the same magnitude (unity) as for the $F = F'$ terms, and roughly the same number of terms are involved. For $F \neq F'$ the energy factors give rise to factors of the form

$$\frac{(m+m')y}{1+[\tau\Delta W/\hbar+(m+m')y]^2} ,$$

whereas the factors of the $F = F'$ terms become

$$(m-m')y/\{1+[(m-m')y]^2\} = y/(1+y^2) .$$

Since $\tau\Delta W/\hbar \gg 1$, and $|m+m'|$ is about $2I+1$ on the average, the $F \neq F'$ factors are smaller on the average by a factor of $(2I+1)\,(\hbar/\tau\Delta W)^2$.

In the experiment the derivatives with respect to y of these energy factors were lock-in detected. On a scale for which the peak lock-in signal at $y = 0$ is unity [from the derivatives of the $y/(1+y^2)$ terms] the contributions of the $F \neq F'$ term are the constant factor $(2I+1)\,(\hbar/\tau\Delta W)^2$. This factor is largest for Ga ($\Delta W/h \cong 2400$ MHz),[19] in which case it is 1.5×10^{-4}. This is at about one order of magnitude too small to be significant in these experiments.

Considering now the nonlinear Zeeman contributions to Eq. (1), it is again the case of Ga that is most severe ($x \cong g_J\mu_B H/\Delta W = 0.092$ at the largest fields and 0.039 at $H = \frac{1}{2}H_{1/2}$). Consequently, Eq. (1) was solved exactly for Ga using the Breit-Rabi formula and standard techniques.[20] This result and the linear Zeeman result were used as $R(y)$ in Eq. (6) and the results compared (by computer). In units where the peak ($H = 0$) derivative signal is 1, the two results differed by 8×10^{-4} at the maximum field (~ 80 G) and $H_{1/2}$ determined as the width between the nulls differed by less than 0.1%. This calculation included the $F \neq F'$ terms discussed above. We nonetheless included the separate discussion of those terms to indicate the reason why negligible changes are to be expected. Order-of-magnitude arguments can also be made concerning the nonlinear Zeeman contribution, but they are more involved and will be omitted.

---

‡Work based on a thesis by Michael Norton submitted to the University of Colorado in partial fulfillment of the requirements for the Ph.D. degree in physics. Supported in part by NSF Grants Nos. GP-8052 and GP-11948.

*Present Address: University of British Columbia, Vancouver, B. C., Canada.

‡Staff Member, Laboratory Astrophysics Division, Natl. Bur. Std., Boulder, Colo. 80302.

[1]W. L. Wiese and A. W. Weiss, Phys. Rev. 175, 50 (1968); and NSRDS-NBS 4, 22 as referenced therein.

[2]B. Budick, *Advances in Atomic and Molecular Physics* (Academic, New York, 1967), Vol. 3, pp. 73–114.

[3]J. K. Link, J. Opt. Soc. Am. 56, 1195 (1966).

[4]E. Hulpke, E. Paul, and W. Paul, Z. Physik 177, 257 (1964).

[5]P. T. Cunningham and J. K. Link, J. Opt. Soc. Am. 57, 1000 (1967).

[6]D. L. Lambert, E. A. Mallia, and B. Warner, Monthly Notices Roy. Astron. Soc. 142, 71 (1969).

[7]G. Breit, Rev. Mod. Phys. 5, 117 (1933); and P. A. Franken, Phys. Rev. 121, 508 (1961).

[8]The corrections to Eq. (2) due to the nonlinear Zeeman effect and the μ, $\mu' = F$, $F+1$ terms are considered in the Appendix, where they are shown to be unimportant for these experiments. The breakdown of the linear Zeeman approximation in the P states need not be considered in the "white-light" approximation since the $\sum_m |m\rangle\langle m|$ in the Breit formula is unaffected. The R_1 and R_2 factors were obtained by summation of terms in Eq. (1), following procedures outlined in Ref. 9. However, a more direct approach is now available in Ref. 10.

[9]A. Lurio, R. L. DeZafra, and R. J. Goshen, Phys. Rev. 134, A1198 (1964).

[10]H. Kretzen and H. Walther, Phys. Letters 27A, 718 (1968).

[11]Natural isotopic abundances were used for the lamps and beams. The nuclear spins of the isotopes do not vary, although the hfs do. Since the Appendix shows that the low-field or linear Zeeman approximation is valid for our measurements, the variations in hfs do not affect these experiments.

[12]The exciting and detected radiation have a finite solid angle so the correct expression for the detected intensity requires integration of Eq. (2) over angles. It can be seen that the amplitude of the symmetric and asymmetric field-dependent terms are determined by this integration, but their forms remain $1/(1+y^2)$. Thus, the actual signals can be interpreted in terms of average or effective angles $\langle\theta\rangle$, $\langle\theta'\rangle$, and $\langle\phi'-\phi\rangle_{av}$.

[13]Further field dependence of the detected fluorescence can arise from attenuation of the initial beam fluorescence by further vapor absorption. Any detailed analysis is complicated by the anisotropy of optical depth in an atomic beam and the complicated scattering geometry. The BAS is intended to represent the over-all consequences of this array of effects whose amplitudes depend quadratically on beam density in the low-density region. For more detailed treatment, see M. K. Norton, thesis,

University of Colorado, 1969 (unpublished).

[14]A. Gallagher and A. Lurio, Phys. Rev. 136, A87 (1961).

[15]Note that the sum on m' in Eq. (4) acts only on the $g_{m'\mu}$. It can readily be shown that $\sum_{m'} g_{m'\mu} g_{\mu' m'}$ in Eq. (2) is zero for $\mu \neq \mu'$ if the detected radiation is not analyzed for circular polarization.

[16]W. Demtröder, Z. Physik 166, 42 (1962).

[17]G. M. Lawrence, J. K. Link, and R. B. King, Astrophys. J. 141, 293 (1965).

[18]N. P. Penkin and L. N. Shabanova, Opt. Spectry. USSR English Transl. 14, 5 (1963); 14, 87 (1963).

[19]Landolt-Bornstein, *Zahlenuverte und Funktionen aus Physik und Chemie* (Springer, Berlin, 1952) Vol. I, pp. 19, 28, 57. The data in this reference were uncertain, so we have used a (10% lower) value based on Eqs. (24)–(26) of Kopferman, *Nuclear Moments* (Academic, New York, 1958).

[20]M. K. Norton, thesis, University of Colorado, 1969 (unpublished).